Metals and Materials International
https://doi.org/10.1007/s12540-024-01646-4

Influence of Patterns on Mechanical Properties of Ultrasonically Welded Joints in Copper Substrate and Wire

Zeshan Abbas[1] · Fan Teng[1,2] · Lun Zhao[1] · Md Shafiqul Islam[3]

Received: 8 November 2023 / Accepted: 29 January 2024

Abstract

Ultrasonic wire welding is considered a method of choice for creating reliable interconnects in electronics industry including aerospace, batteries and electric vehicles. In this paper, ultrasonic welding tests between EVR252 copper wire and substrate are carried out. Novel pattern morphologies are machined on substrates to explore its influence on mechanical properties of welded joint. Patterns are divided into three different categories e.g., original surface, vertical and horizontal shapes. Cracks, microstructure strength and tensile properties of welded joint are studied and its joining mechanism is analysed. Compared with the reference substrate (S1), the welded joint performance of the longitudinal patterns (S2, S3, S4) has been improved, among which the longitudinal pattern (S4) has the most significant improvement (+ 15%). Likewise, the performance of transverse pattern (S5) welded joints is relatively poor (− 16%). The microstructural analysis using SEM has revealed predominant joint strength on Cu wire surface while maintaining rock-like and compact properties of S4 substrate. Upper side of wire-harness compactness is frequently observed due to vertical direction of patterns on substrate and also increases the strength of welded joint. Values of failure load, failure displacement and failure energy absorption were increased by 7.9%, 72% and 35% for S2, 6.1%, 75% and 42% for S3 and 15%, 87% and 113% for S4 compared to S1. Failure modes of welded joints are mainly characterized into: 1-poor ductility or rupture (no deformation) failure in vertical 3-line pattern joints 2-cylindrical deep holes failure in vertical 3-line zigzag pattern joints and 3-bulging effect failure in horizontal 3-line zigzag pattern joints. Point and line scans EDS measurement were performed to investigate weaker and stable trends of different locations in welded joints. In S4 substrate, 17.9% carbon content at the position of welded joint was investigated, leading to content of less oxides and fraction impurities. However, S1 weld zone contains 38.7% carbon content which can weaken welded joint and reduce durability.

Keywords Ultrasonic welding wire harness · Machined patterns · Copper substrates · Failure and strength analysis · SEM and EDS analysis

1 Introduction

Many advanced electronic components require wiring-harness connections in the context of dual carbon with the rapid development of new energy vehicles [1, 2]. Therefore, the demand for certain products has largely shaped the route. The process of manufacturing wire-harnesses consists of precisely connecting cables to terminals and insulating elements in a way that allows current to flow from one point to another. A wire-harness assembly refers to a unified collection of wires, cables and connectors that are joined together to facilitate the transmission of electrical signals and power between various components of a machine or system [3]. This process may include wire bonding, brazing, clamping, laser welding, gluing, friction stir and other fusion bonding

Zeshan Abbas and Fan Teng have contributed equally to this work.

✉ Lun Zhao
zhaolun@szpu.edu.cn

[1] Institute of Ultrasonic Technology, Shenzhen Polytechnic University, Shenzhen 518055, China

[2] School of Mechanical and Control Engineering, Guilin University of Technology, Guilin Guangxi 541004, China

[3] Department of Mechanical Engineering, Blekinge Institute of Technology, 37179 Karlskrona, Sweden

Published online: 09 March 2024

methods of connecting wires e.g., ultrasonic welding [4, 5]. The clamping is a mechanical connection in which plastic deformation is produced by applying a certain mechanical pressure. The clamping is used to fasten two metals together. More, the pressure is applied between the wire-harness and the terminal by means of clamping devices [6]. Laser welding is a highly efficient and sophisticated welding method that uses the heat generated by a high energy density laser beam bombarding the weld specimens to weld stable joints [7]. Brazing is a method of joining workpieces using a metal with a lower melting point than the base material. The bonding of the material begins after the workpiece is heated. Moreover, the brazing material at a high temperature is joined together between the high strength level and melting point of the adhesive material [8, 9]. The liquid brazing material is used to wet the base material to fill the joint gap and diffuse with the base material. Friction stir welding uses the heat generated by the contact surfaces of the workpieces rubbing against each other as a heat source [10–12]. The method of welding with plastic deformation of the workpiece under pressure changes the state of the metal. Therefore, there are several variants of friction welding depending on the process and equipment such as linear friction welding, rotary friction welding and inertial friction welding [13]. Friction stir welding is also considered one of the variants originating from the friction welding process, which is currently common for joining complex and rigid materials [14]. The traditional mechanical connection and welding may have high contact surface resistance, low connection strength, slagging, porosity, large deformation and other crack defects [8, 15]. The ultrasonic metal welding is the joint action of welding static pressure, ultrasonic high-frequency vibration and high-frequency friction at the materials interface during the welding process [16]. Hence, it turns out to produce a high degree of plastic deformation and rapid temperature rise. It breaks down and removes the oxide film and contaminants at the interface of specimen. The pure bare metal atoms come into contact and form a welded joint in the form of a metallic bond [17]. It has the advantages of low cost, high efficiency, high stability, no damage to non-welded areas, high efficiency, no pollution effects, low deformation of the workpiece and automation compared to traditional techniques such as mechanical joining and welding [9, 18]. This is why it is widely used for connecting wire harnesses to substrates and wire harnesses together with terminals.

The traditional connection of wiring-harness and substrates has found flaws and defects in appearance (e.g., fracture nucleation at interface, joint instability and grooves), lack of bond strength and increased internal resistance due to the generation of junction compounds [7, 19]. Aluminum wire-harness is likely to corrode more when used to weld with connectors. So far, some researchers have carried out particular studies on ultrasonic welding for wire-harness and substrate connections. However, the most of them had worked on the process parameters to explore the effect of welding parameters on joint morphologies [20, 21]. For example, Metheny et al. investigated the effect of welding pressure and welding amplitude (%) on the strength of ultrasonic joints in single-core multi-strand cables. The study found that the higher applied pressure creates higher the maximum fusion strength. Likewise, the higher the applied pressure and amplitude (%) produces the formation of a weak joint under the lower welding energy [2]. Liu et al. determined that the welding parameters on the mechanical properties of copper and aluminum joints were in the main influence order of energy > pressure > amplitude (%) through orthogonal experiments. So, interface fractures in a mixed tough-brittle mode were further investigated [22]. Li et al. studied the relationship between the tensile strength of Cu and Al cables that were ultrasonically welded. The welding energy revealed that the tensile strength would first increase with increasing energy and when it reached a peak, it would then decrease with further increase in welding energy [23]. Andreas et al. studied the ultrasonic welding of EN AW-1070 cables with EN CW004A substrate and investigated that the strength of the welded joint increases with welding time [3]. It further determined when the time reaches a peak and then the strength decreases instead of increasing with welding time [24]. Kang et al. studied the ultrasonic welding of 1.2 mm copper wire to 0.3 mm thick copper sheet. The study discussed the optimal welding parameters such as welding pressure of 4 bar, welding amplitude of 75 and welding time of 4 s [25]. Lu et al. found that the optimal welding parameters for ultrasonic welding of copper cables and substrate (10 mm^2) e.g., time of 0.8 s, amplitude of 62.4% and pressure of 4 bar [26]. Kumar et al. investigated the welding of Al cables and copper substrate. The study described the addition of Ni coating that would avoid the formation of intermetallic compounds or eutectic layers in the bonding region resulting in good tensile joints [27, 28]. Kitaura et al. studied Al wire harnesses which were bonded to copper substrate. The results explored the effect of different terminal surfaces on their welded joints. The study determined that different surface roughnesses had a greater effect on the tensile strength of joints with raised surfaces loaded by up to 48% compared to original terminals [29]. Singh et al. studied the effects of applied load, surface roughness, welding power and welding time on joint strength. The tensile strength varied with welding time [30]. Pascal et al. proposed influence of different surface conditions on mechanical properties during ultrasonic welding of Al wire strands and Cu terminals [31]. Khalifa et al. Performed experimental investigation of joints strength obtained by ultrasonic welding and soldering under pure T-peel tests using DIC method [32]. Hewan carried out et al. orthogonal experiments and bonding analysis of ultrasonic welded multi-strand single core copper cables [33]. Fuxing et al. investigated joints formation and bonding mechanism

of ultrasonic welded multi-strand single core copper cables with copper terminals [34].

The strength profile increases to a maximum value and then decreases at fracture regardless of the roughness value and applied load [35]. It was concluded that the contact temperature plays an important role in the initial bond strength throughout the study. The bond strength is mainly controlled by the surface roughness in the final stage. However, there have been a number of researchers who have conducted numerous studies on the ultrasonic welding process, but most of them belong to the study of connection between two metal plates. Therefore, the research on wire-terminal harness with substrates connection is relatively insufficient and most of the research is directed at the influence of welding parameters [36, 37]. The copper wire and pure copper plates are widely used in manufacturing industry (e.g., automobiles and aircraft) due to its tremendous performance characteristics of electrical and thermal conductivity. However, there are few research studies available on ultrasonic welding between copper wire and pure plate.

In this study, ultrasonic metal welding between Cu wire and pure Cu plate is carried out. The microcracks, gaps/voids, microstructure strength and tensile properties of the welded joint are studied and its joining mechanism is analyzed. Similarly, three different vertical patterns and one horizontal pattern were machined to create the welded joint on the substrate and wire harnesses. Likewise, one of the substrates from the five samples is designated as the reference substrate which is processed without a pattern on the surface. The accuracy of the patterns is gradually verified. At the same time, SEM microscopic analysis of various pattern surfaces (e.g., forming quality analysis, wire failure analysis and joint strength analysis) was performed. Finally, EDS analysis of point and line scans was performed to investigate the weakest and most consistent trends of different locations in the welded joints.

2 Materials and Experimentation

2.1 Materials and Samples

The EVR252 shielded high voltage wire and T2 purple copper material were selected for the experiments. The EVR shielded high voltage wire has excellent electrical conductivity, high temperature and high voltage resistance extensibility. It is further widely used in new energy applications such as automobiles and aircraft. In addition, T2 copper is used which has good electrical conductivity, ductility and machinability. This is widely used in battery plugs, generators and other applications. The elemental constituents of the both materials are given in Table 1. The process parameters used during the ultrasonic wire harness welding are shown in Table 2.

The leading substrate (S1) is the original unprocessed copper sheet which is used as a reference to compare with the processed substrates. The S2 copper plate has three vertical stripes/lines and the width of each stripe is 1 mm. Similarly, the distance between each strip is kept at 1 mm. The S3 copper plate has three vertical line zigzag structures and the width of each stripe is kept at 2 mm. Moreover, the distance between each strip is kept at 1 mm. The S4 copper plate has vertical five-line structures with a width of 1 mm and a space of 1 mm between each line strip. Likewise, the S5 copper plate has horizontal lines combined with three lines including zigzag patterns which collectively named straight-curved patterns. So each strip is kept at 1 mm width and each strip is 1 mm apart. Figure 1a displays the different types of machined substrates (S2–S5) and reference substrates (S1) which are soldered with EVR252 shielded high voltage copper wire. Figure 1b shows the original copper substrate containing machined patterns on the surface. The schematic and experimental setup of ultrasonic welding wire harness process is shown in Fig. 2. Figure 2a demonstrates the schematic of ultrasonic welding wire harness and its working principle. Figure 2b shows the experimental setup of ultrasonic welding (D01, HMS, and China) process for copper wire and substrates. The results of SEM and EDS (JSM-IT800 (SHL), JEOL and Japan) were obtained to perform the surface analysis of the various patterns [38]. An ultrasonic harness welding machine with a frequency of 20 kHz and a welding head width of 13 mm was used. The length of the horn was 10 mm. Furthermore, the material characteristics of the EVR shielded high voltage wire with T2 copper are shown in Table 3.

Table 2 The process parameters used during ultrasonic metal welding process

Welding parameters	Values
Pressure (MPa)	0.26
Vibration amplitude (%)	85
Welding energy (J)	6000

Table 1 Chemical composition of the selected materials (%)

Content	Element					
	Cu	O	Fe	Bi	Pb	S
Copper wire	≥ 99.95	≤ 0.03	≤ 0.004	≤ 0.003	≤ 0.005	≤ 0.0015
Copper terminal	≥ 99.90	–	≤ 0.005	≤ 0.001	≤ 0.005	≤ 0.005

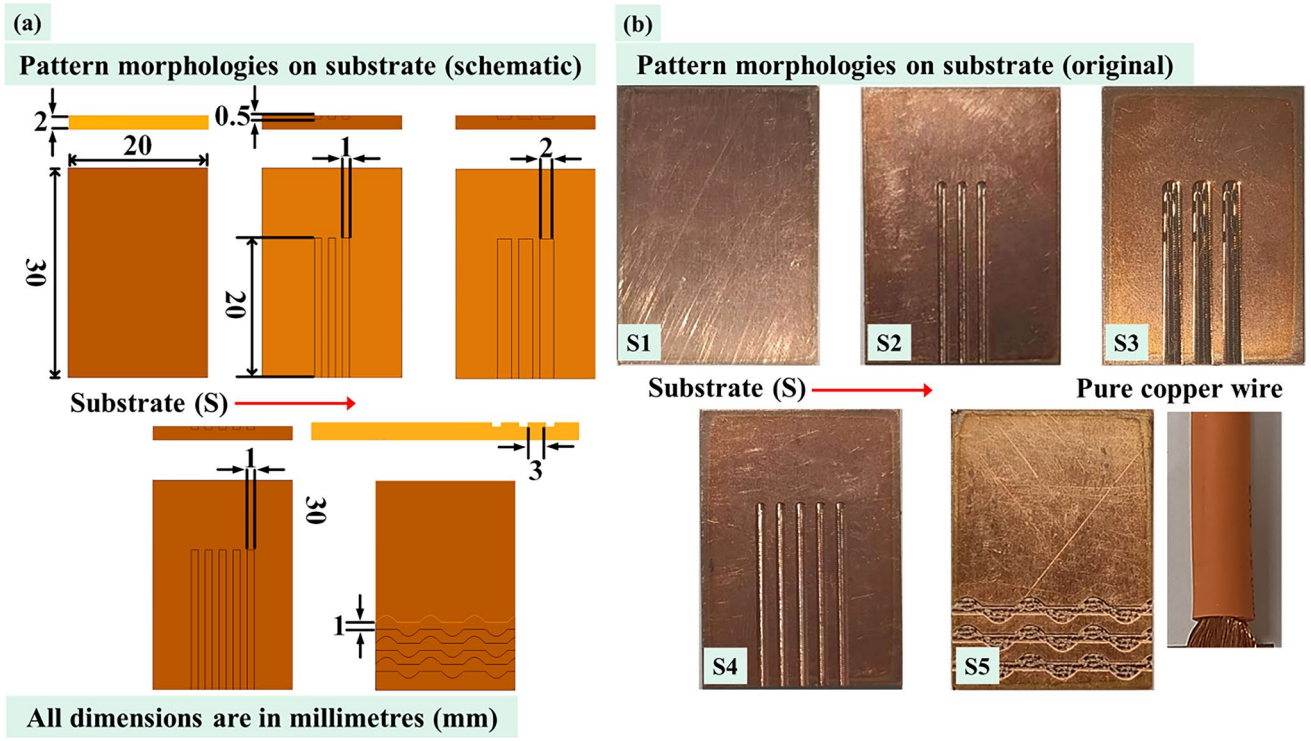

Fig. 1 Schematic and original pattern morphologies on copper substrate used in ultrasonic welding wire harness: **a** schematic photograph of patterns **b** the original copper substrate containing machined patterns on the surface

2.2 Methods

Two discrete techniques have been applied to characterize the mechanical properties, interface failure, tensile failure form, elementary fracture analysis and joint microstructure analysis, namely ultrasonic welding of wire harness, T-peel testing and SEM & EDS analysis in this experimental work. In order to explore whether there are other ways to enhance the mechanical properties of welded joints besides welding parameters, the several pattern designs were carried out on the Cu substrate. Thus, three patterns of S2, S3, and S4 are consistent with vibration direction of the welding head. Furthermore, S2 and S3 are designed to explore whether the pattern width has an impact on the joint strength. The S5 pattern is perpendicular to the vibration direction of the welding head, and S2 and S5 are used to explore whether the pattern direction affects the joint strength.

2.3 Ultrasonic Welding of Wire Harness

The welded joint formation during the ultrasonic welding of wire harness is divided into the following stages:

In the beginning, the materials are prepared to apply for the ultrasonic welding wire harness. It is considered as the first stage of the ultrasonic welding process. The second stage of the workpiece after the completion of clamping is subjected to the downward pressure of the tool head. So, the wire/cable and the substrate are exposed tightly in contact. In the third stage, when the pressure reaches the pre-value then the tool head will produce high-frequency ultrasonic vibration, which makes the two workpieces in relative motion. Meanwhile, the cable and the substrate surface oxide will break off and fall on to the ground. In the fourth stage, the two workpieces gradually change from point contact to line contact and then to surface contact. The mechanical vibration of the workpiece is converted into plastic flow, frictional work and heat energy at the interface under the combined action of high-frequency ultrasonic vibration and static pressure. The interface atoms are mutually activated and dispersed to achieve solid-state bonding of the workpiece during ultrasonic wire harnessing. Figure 3 illustrates the various steps of the ultrasonic welding wire harness.

2.4 Analysis of Tensile Shear Test

The tensile strength of ultrasonic welded joint is an imperative index to evaluate the quality of the welded wire joint. Therefore, MTS universal experimental drawing machine (CMT4304, MYS, and American) was used for tensile shear test analysis. The welded parts are stretched according to USCAR-45 standard. For each surface condition, 10 samples were used for tensile test in each group. In particular, the

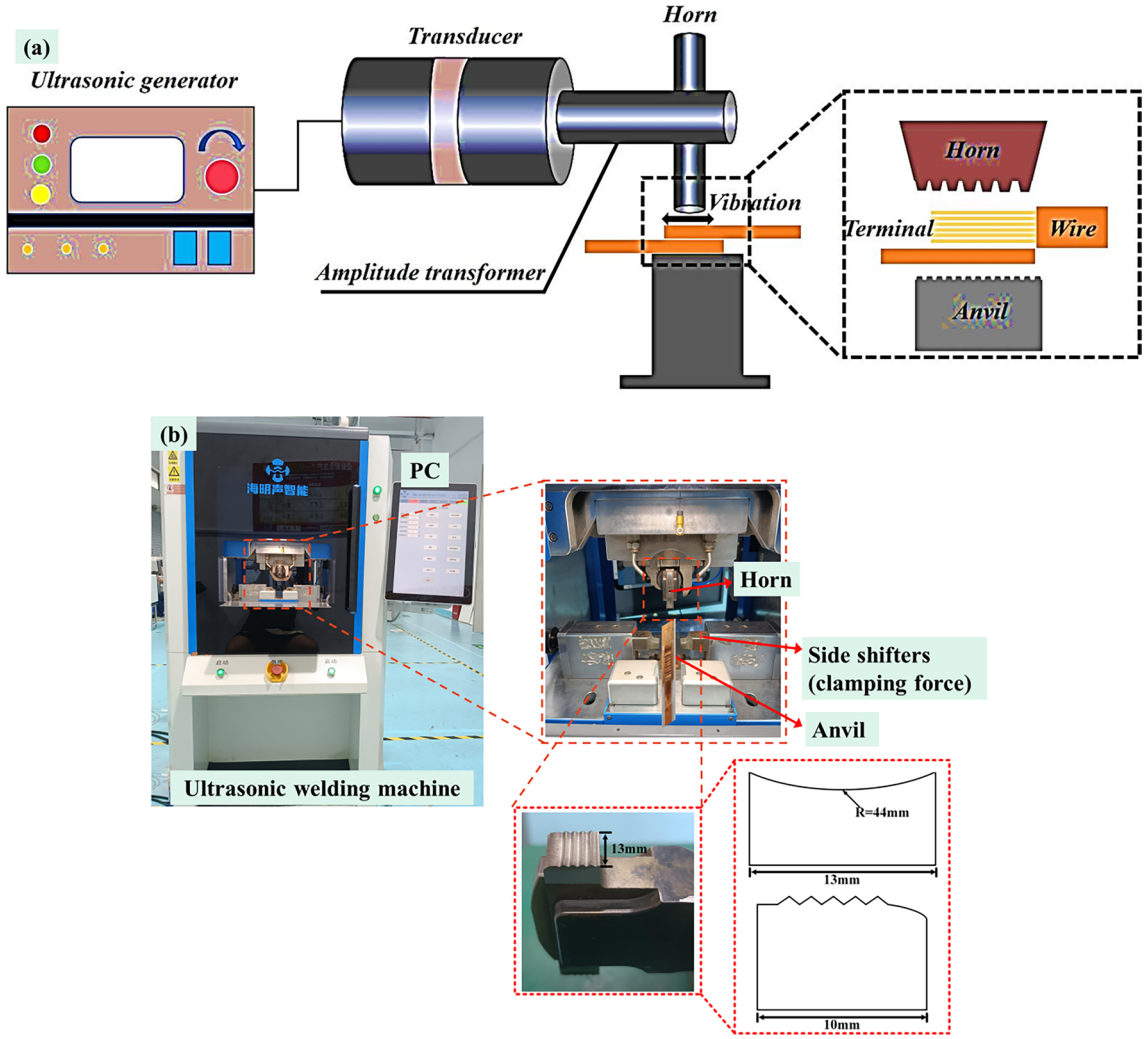

Fig. 2 Schematic and experimental setup of ultrasonic welding wire harness process: **a** schematic of ultrasonic welding wire harness process and **b** photograph of USW machine coupled with the horn and anvil specification

Table 3 The properties of EVR high voltage shielded wire with T2 copper material

Materials	Tension strength	Yield strength	Elongation	Modulus of elasticity
	σ_b (MPa)	σ_s (MPa)	δ (%)	E (GPa)
EVR high voltage shielded wire	200–300	33	≥ 35	128
T2 copper	200–204	60–70	≥ 30	119

tensile speed was maintained at 1 mm/min. So, the comparison of the maximum and minimum welding strength of different substrates (S1-S5) during tensile test is shown in Fig. 4. Figure 5a shows the test setup of the combined tensile and shear test, where 6 appropriate specimens were taken from each set to represent the tensile strength of the specimens. Likewise, Fig. 5b demonstrates 10 specimens tested of each versatile pattern on the substrate which is welded with copper wires.

3 Results and Discussion

3.1 Mechanical Properties Analysis of Welded Joints

Figure 6 illustrates the analysis of mechanical properties of the terminal-harness joints (e.g., tensile peak average load, failure average displacement and failure energy absorption). The direction of the pattern on the terminal surface has a significant influence on the joint strength of each sample. The transverse pattern on the terminal surface will lead to lower

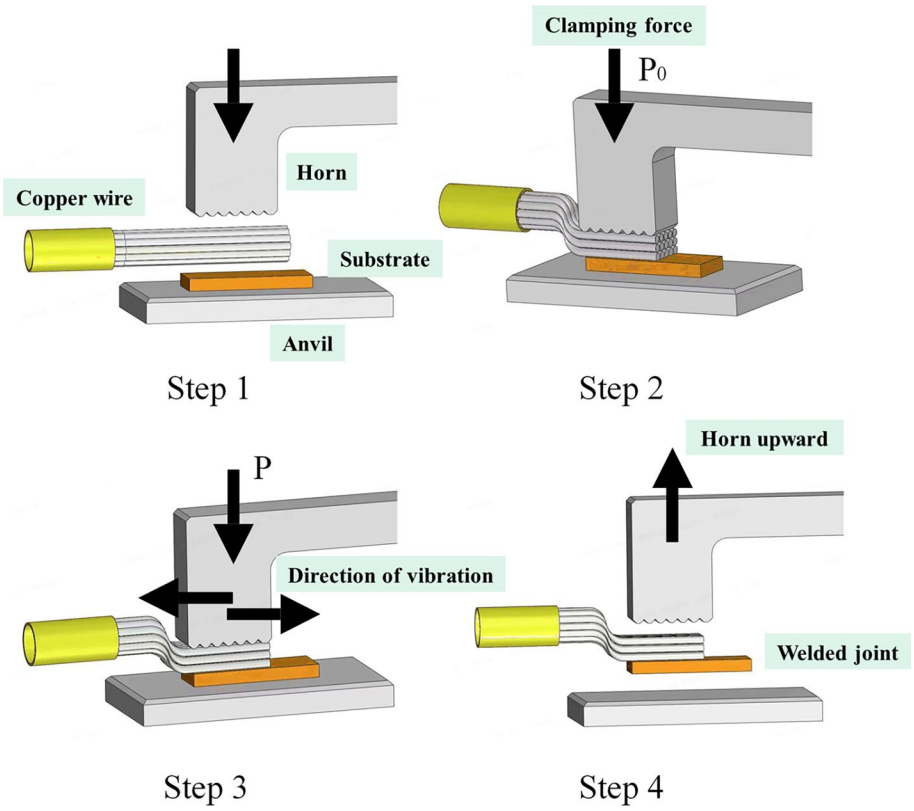

Fig. 3 The ultrasonic welding wire harness process: (step1) apply clamping force (step2) initiation of vibration (step3) evolution of deformation layer and (step4) welded joint and top mounted horn

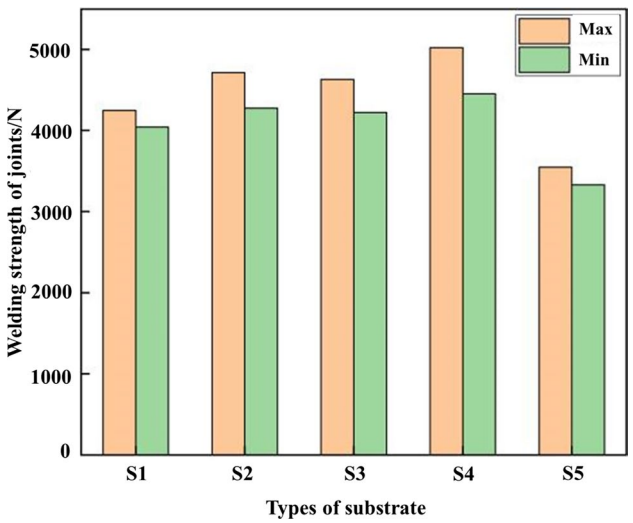

Fig. 4 The comparison of welding strength of different substrates (S1–S5) during tensile test

failure load, failure displacement and failure energy absorption value. The average failure load, failure displacement and failure energy absorption values of specimen S5 are solitary 3461N, 9.8 mm and 30.86J, respectively. However, the failure load is still high according to the USCAR-38-1 performance requirements for the tensile strength of 25 mm^2 copper wires (1350N). The average failure load and failure displacement of the original surface sample S1 are 4136N and 16.7 mm, respectively. Likewise, the values of sample S5 (1 mm) are compared with sample S1. The failure load, failure displacement and failure energy absorption values are reduced by 16%, 41% and 30%, respectively. Similarly, the transverse pattern reduces the mechanical strength of the specimen joint. The vertical pattern on the terminal surface has a remarkable effect on the failure load and failure displacement of the specimen. The failure load, failure displacement and failure energy absorption value increased by 7.9%, 72% and 35% (S2), 6.1%, 75% and 42% (S3) and 15%, 87% and 113% (S4) as sample S1 is compared to S2 (1 mm), S3 (2 mm) and S4 (1 mm). This is due to the direction of vibration of the welding head that is in line with the vertical pattern and direction of laying the copper wire. The copper wire and terminal have more and sufficient friction when these are soldered. The connection is more sufficient, so its mechanical performance will be better than that of the horizontal model.

The results indicate that the vertical pattern on the terminal surface can improve the joint strength of the sample. The influence of the pattern width on the terminal surface and the number of pattern bars on the joint performance of samples were investigated for samples S3 and S4, respectively. The values of failure load, failure displacement and failure energy absorption of sample S3 (2 mm) are 4387N, 29.2 mm and 43.93 J, respectively as shown in Fig. 6a–c.

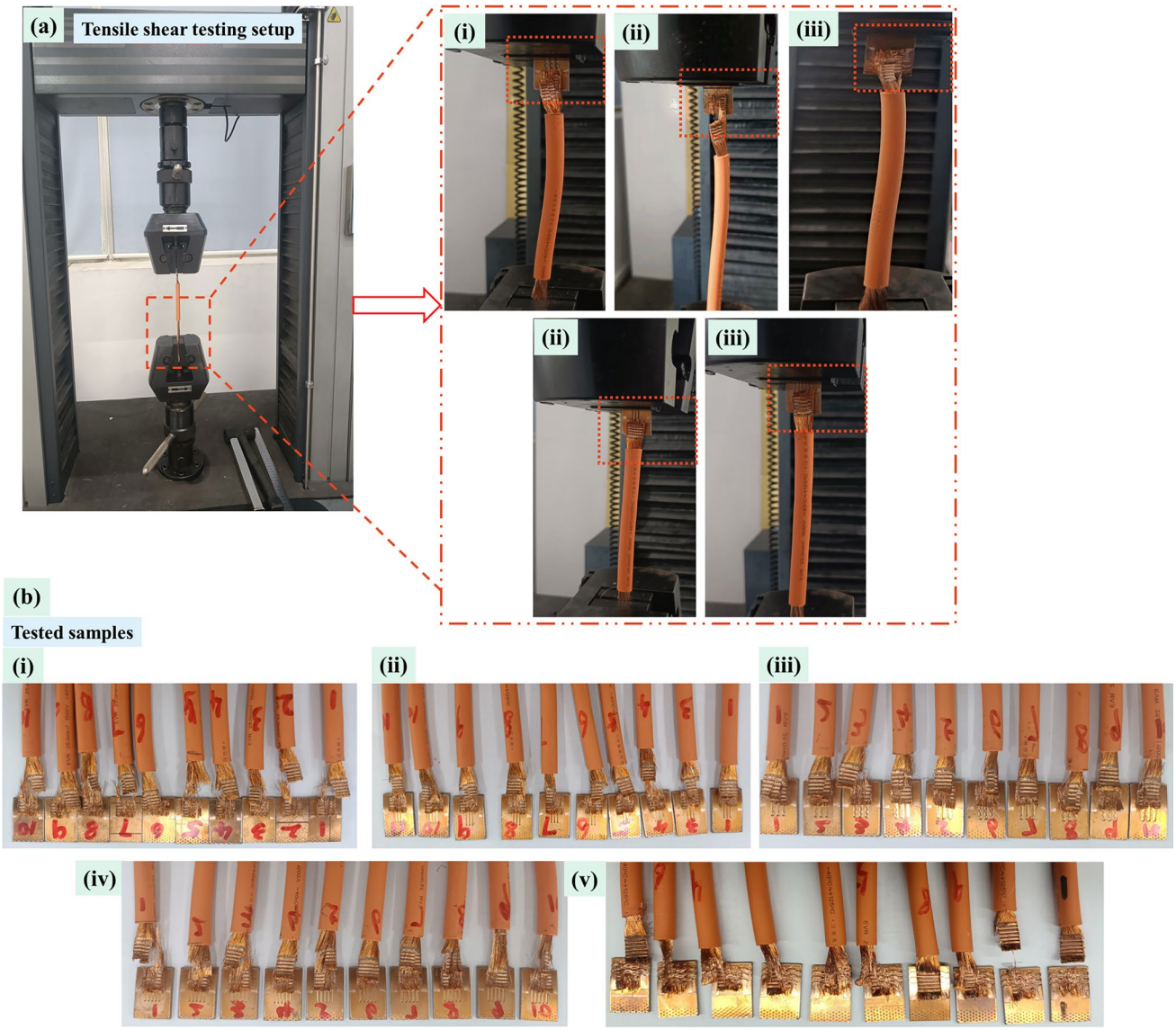

Fig. 5 The tested samples: **a** test setup of combined tensile and shear test and **b** various tested specimens welded with substrates containing versatile surface patterns

The results showed that the values of machining parameters are not different from sample S2. Therefore, the pattern width has no significant effect on the joint strength of specimen. Equally, S4 (1 mm) has increased the number of patterns compared to S2 (1 mm) and its failure load, failure displacement and failure energy absorption values are 4755N, 31.2 mm and 35.84 J. The failures are increased by 6.6%, 9.6% and 35.84 J, respectively to compare with sample S2. The welding area is increased by 58% thru increasing the number of ribs which are equivalent to maintain the welding area. Therefore, this is the main reason for improving joint strength.

3.2 SEM analysis of Substrate-Wire Harness Joint

3.2.1 Forming Quality of Substrate-Harness Joint

In this study, the joint holes mainly appear in the copper wire part because the joint forming process slowly forms mechanical fit from welding head part to terminal direction. The gap between the copper wires will affect the strength of copper wires and the substrate. During the stretching process, the parts that have not formed a good connection may fail first such as the joint tearing shape. The voids created on the surfaces of substrates are called bugholes or simply

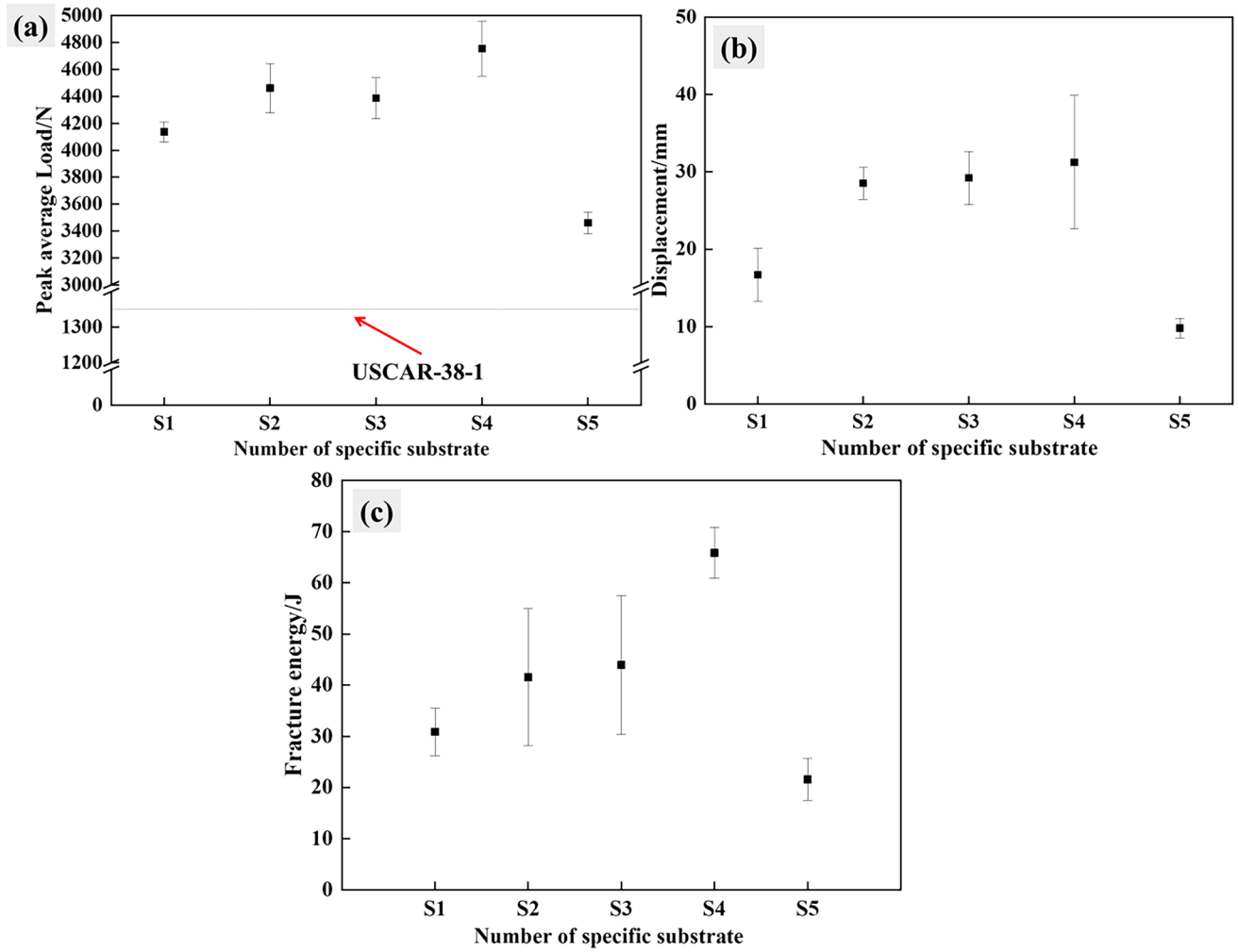

Fig. 6 Test analysis of mechanical properties of the terminal-harness joints: **a** average peak load **b** average failure displacement and **c** average energy absorption

surface voids. These defects appear as regular or irregular pits with diameters ranging from a few micrometers to 1 mm in diameter. Randomly generated cracks regularly spread across the surface to create small holes at random locations in the substrates and cause weld joints to break. Figure 7 displays the cross-sectional view of vertical and horizontal lines joint. Figure 7a, b represents a cross-sectional view of S1 and S5 welded joints (see Part A). It is determined that there are some random gaps on the soldered surface of S5 joint when the copper wire and the terminal surface are ultimately connected and welded. Figure 7a displays that there are a large number of tiny copper wires and pattern pieces in sample S5. So there is a very small and thin joint due to the creation of voids on the surface which reduces the bonding area. The random cracks originate at the surface of the substrate, which weaken the joint and ultimately reduce the tensile strength. Similarly, the 1 mm line on the surface produced several broken holes. During SEM analysis, the zigzag shape of the voids was observed. The minimum hole size in a trench was approximately 50 µm on the joint surface. Besides, a very long white space was observed during the analysis which could lead to a decrease in the life of the joint and also weaken its strength. The gaps between copper wires can be eliminated. By appropriately increasing the welding parameters, the copper wires will be more tightly bonded. However, excessively high welding parameters will cause over-soldering, which will reduce the strength of the joint. Figure 7b shows a reference substrate copper wire and patterns on sample S1. The spaces and fracture surface are not available under large surface area. However, a few random gaps are formed, but most of the area is properly welded which shows the compact and solid surface of the substrate. In addition, the degree of compression of the welded joint between Cu wire and the pattern is also slightly lower. This must be due to the large amount of gaps between Cu wire and the terminal by reducing the length of copper

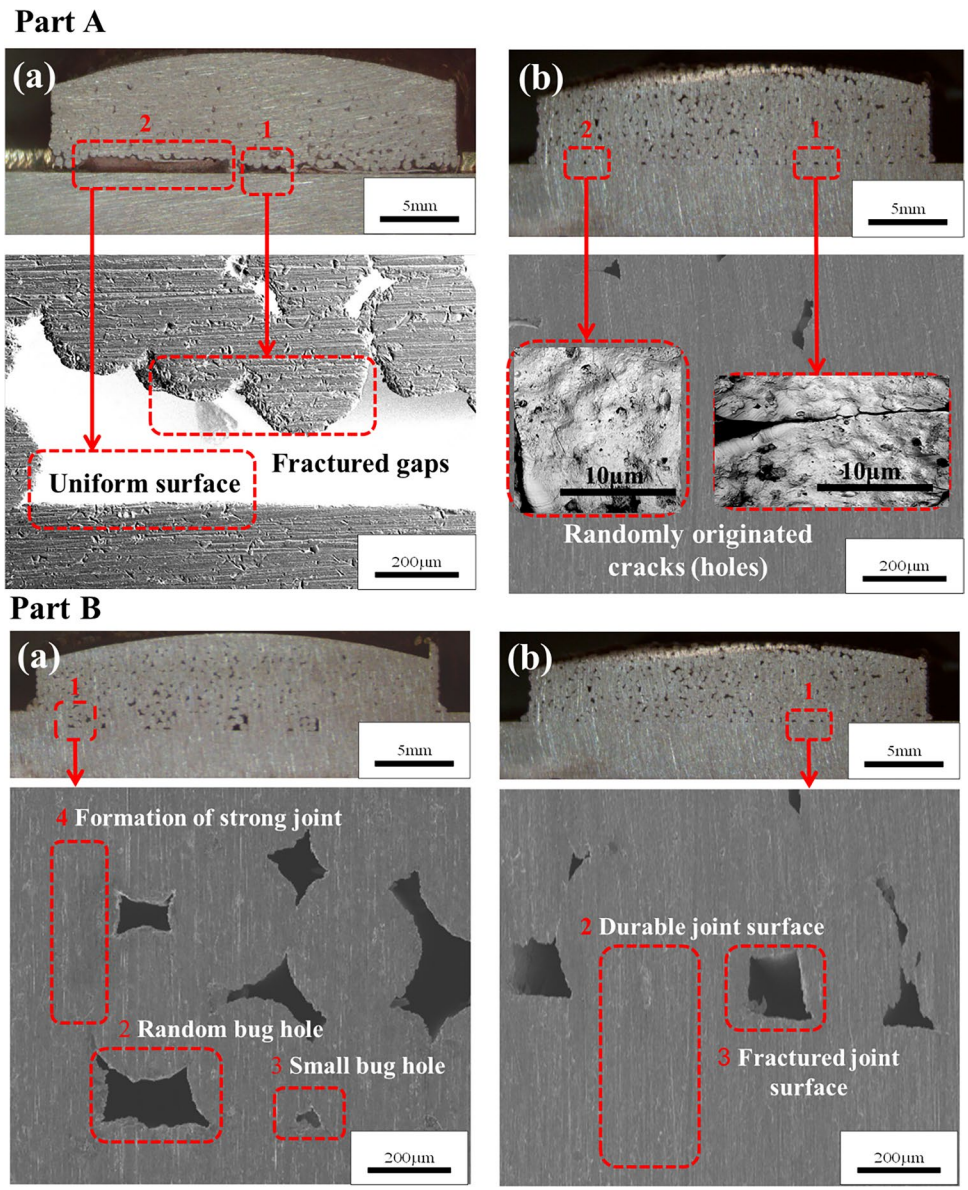

Fig. 7 The cross-sectional view of vertical and horizontal lines joint: Part A **a** Optical microscope overview of the sample (S5) demonstrating fractured voids and **b** Optical microscope overview S1 which provides the detailed view of random cracks on the surface. Likewise, Part B **a** S4 optical microscope overview demonstrating small and large random bugholes as well as strong joint formation surfaces and **b** S1 optical microscope overview, which provides the detailed view of a few fractured side and more area is covered with durable and stronger bonding surface

wire. The relative movement between the wire and terminal reduces the plastic deformation of copper wire. Therefore, the reduction of the bonding area and reduction of relative motion lead to weakening of the joint mechanical properties in S5 sample.

Figure 7 demonstrates a cross-sectional view of joints S1 and S4 (see Part B). The degree of surface connection of the copper wire and terminal is almost the same as that of S1 as shown in Fig. 7a, b. However, a tight bond is formed between the copper wire and pattern side in S4 substrate as shown in Fig. 7b. Thus, it increases the mechanical properties of welded joint in S4 sample by increasing the total surface area of joint. The results obtained from S4 showed several giant bug holes on the surface. These bug holes can quickly break the welded joint and also reduce the life of the joint. Likewise, the surface of S4 substrate is very smooth and rock-like shape which makes the bond sturdy on that side. Finally, the tensile strength does not change abundantly. Similarly, the 1 mm line on the surface of S4 has produced several large bugholes. During SEM analysis, the shapes of insect holes were observed to be rhomboid. The minimum rhomboid bughole size was approximately 70 μm on the surface. Equally, a very long gray colored area was observed to indicate the smoothness and compactness of the surface which could increase the lifetime of the joint and also make it stronger. Figure 7b displays a sample S1 which is essentially a reference substrate without surface patterns. The bug holes and fracture surfaces are not omnipresent under the large surface area. However, there are few tiny bugholes and different shapes were found on upper surface of the substrate. Most of the area is properly welded which produces a stable and durable joint surface. Bonding on the

S1 substrate generates fewer bugholes compared to S4 and S5 substrates.

3.2.2 SEM Failure Mode Analysis

Fractography is a technique which is applied in failure analysis to study different types of fracture surfaces in different materials. Fractured surfaces assist to determine the cause of failure in an engineered product when subjected to SEM analysis. Figure 8 illustrates the different types of unusual failure mode (e.g., generation of deep holes, poor ductility of the material and development of bulging effect) during ultrasonic welding of copper substrate and wire. A series of experiments were conducted to achieve the best quality solder joint of the substrate and the copper wire under optimal processing parameters. The constant processing parameters (e.g., pressure = 0.26 MPa, amplitude = 85%, and welding energy = 6000 J) were used during the welding process of different substrate harness specimens based on the machined patterns. Figure 8a illustrates the analysis of the failure mode that occurred on substrate S2. The sectional view of the three-line vertical patterns (S2) is shown in Fig. 8a. The fractography analysis shows that the welded joint between the copper wire and the substrate is not productively and well-formed based on the machined patterns. The orientation of the joint is inappropriate and produced deep holes during shrinkage between the two surfaces of the specimens. The SEM results showed that the shape, orientation and dimensions of the vertical three-line patterns are not enough saturated. Therefore, the copper wires float on the surface of the substrate. The wire harnesses are not exactly in focus when the specimen is placed in the correct direction. Although, the shape and orientations were specified during the processing of the patterns, but the length of the copper wires was interrupted by the depth of the vertical patterns. Therefore, the surface of the model has voids which propagate the deformation in the joint of two similar metals and reduce the strength of the welded joint. The welding strength of the joint in S2 decreases significantly under constant process parameters. The maximum welding strength of the joint was reached 4712.65N and the minimum force was obtained 4275.5N under the testing of 10 samples with a series of ultrasonic welding experiments.

Since, failure modes of joints S1, S2, S3, S4 and S5 have all been investigated and occurred due to pull-out failures of the joints. The failure joint S2 is selected for the plastic deformation analysis as shown in Fig. 8b. The copper wire has obvious necking phenomenon which indicates that the copper wire has undergone plastic deformation. Likewise, plastic deformation is the permanent distortion that occurs when a material is subjected to tensile, compressive and torsional stresses after exceeding its yield strength and causes it to elongate, compress, bend and twist. The experimental results in this work investigate that there is a brittle fracture in the copper wire which may be due to high welding temperature during the welding process. This further causes a small portion of copper wire to undergo phase transition behavior at the substrate surface. Therefore, it has been investigated that it increases the brittleness of wire in particular edges.

Figure 8c illustrates the analysis of the failure mode in substrate S3. The cross-sectional analysis of the vertical three-line zigzag patterns (S3) was investigated which generated the zigzag junction morphology in copper wire. The processing parameters were kept constant. The consequence was similar as produced in case of S2. From the failure mode results, it can be observed that welding energy (6000J) and clamping pressure (0.26 MPa) had the greatest influence followed by amplitude. The welding strength of welded joint was reduced in zigzag shape of the pattern due to influence of welding energy. The zigzag shape surface illustrates the poor and ductile formation of welded joint. So, it may not be deformed and may break with low welding strength. Therefore, the welding area between Cu wire and Cu substrate was spongy and weakly ductile. Similarly, the welding strength of the joint on the surface of S3 is reached in normal amounts under constant process parameters. The maximum welding strength of the joint was achieved 4630N and the minimum force was reached 4222.2N under the testing of 10 samples with a series of ultrasonic welding experiments.

Figure 8d demonstrates the failure analysis originating from substrate S5. The cross-sectional analysis of horizontal three-line zigzag patterns (S5) exhibited a weak joint morphology. The horizontal lines of the patterns are not tightly constrained due to parallel morphology of the pattern lines. The horizontal line patterns are used to produce bulging phenomenon in the welded joint area. The connection near the wires was made in a coarse size due to absorption of low welding energy. Likewise, poor welding strength is achieved in welded joint at S3 under constant process parameters. The maximum welding strength of the welded joint was reached 3524N. The minimum force was obtained 3330N under the testing of 10 samples with a series of ultrasonic welding experiments. The results showed that low welding energy absorption can produce a weaker welded joint in horizontal line patterns. The study showed that the failure is possible in three different ways as follows: (1) poor ductility or rupture (no deformation) failure in the vertical three-line pattern joints. (2) cylindrical deep holes failure in vertical three line zigzag pattern joints. (3) bulging influence failure in the horizontal three-line zigzag pattern joints.

3.2.3 SEM Strength Mode Analysis

The strength mode analysis provides advantageous and straightforward information of substrate-wire welded joint

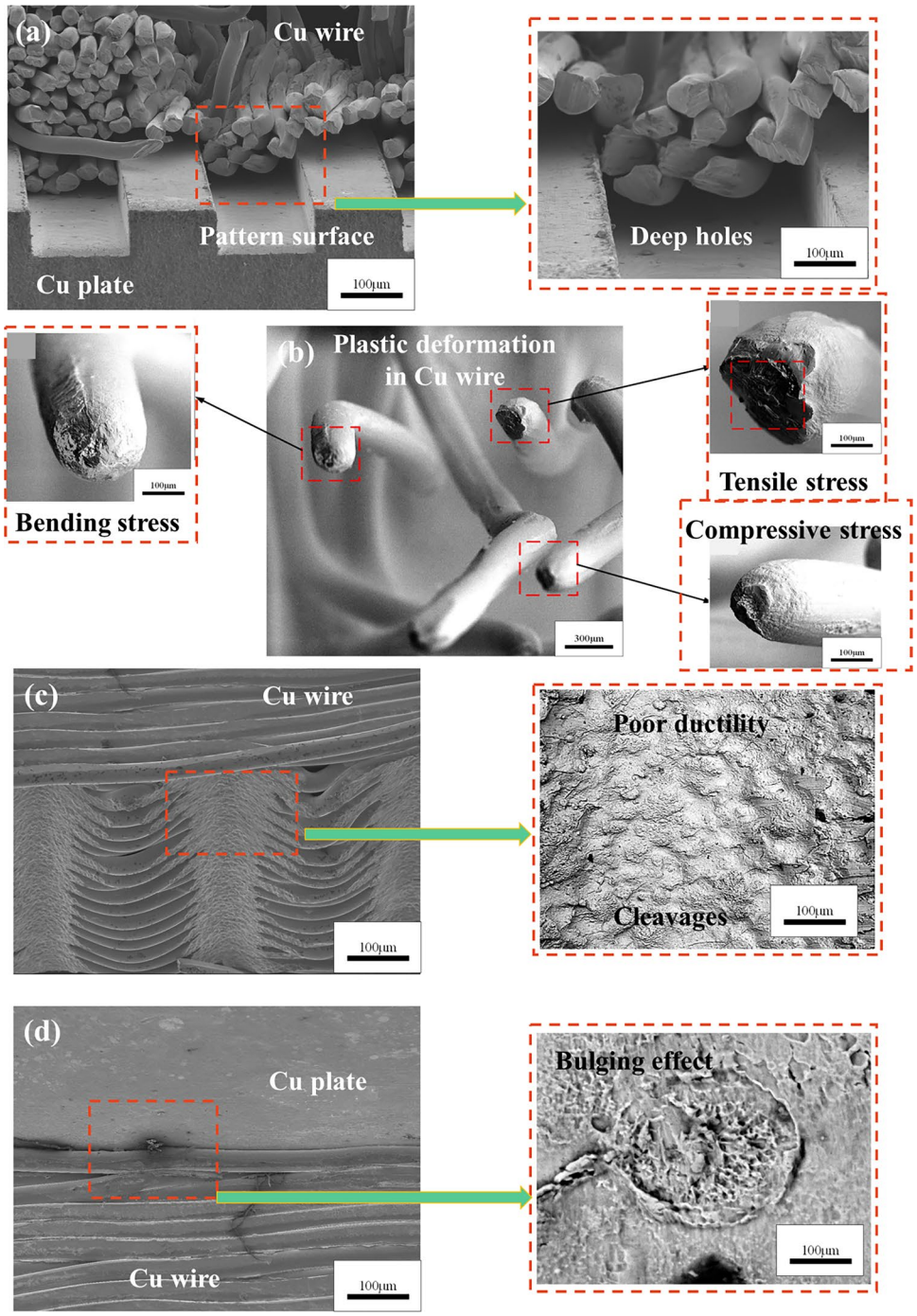

Fig. 8 Fractography with SEM test analysis of different substrates to wire harness: **a** cross sectional analysis of vertical three-line patterns (S2) **b** cross sectional analysis of copper wire **c** cross sectional analysis of vertical three-line zigzag patterns (S3) and **d** cross sectional analysis of horizontal three-line zigzag patterns (S5)

for better interpretation of bond strength results. The main points of SEM analysis for strength mode are as follows: (i) non-glutinous strength (ii) mixed strength (iii) resilient property (iv) denseness or compactness and (v) inflexibility. Figure 9 illustrates the strength mode analysis originating from substrate S4. The cross-sectional analysis of vertical five-line patterns (S4) exhibited a strong and stable joint morphology. The SEM analysis of the joints on five-line patterns (S4) displayed a compact and hardened microstructure. The micropores and tear edges were appeared in the wire harness zone. Thus, the deformation of the wire surface was quite severe. The cutting edge of the welded joint was clearly visible in the microstructures. It belongs to the aggregate of micro-wires to investigate the internal morphology of the welded joint. The analysis investigated that the sizes of the thermally solidified zone and the reaction layer are two key factors that control the strength of the welded joint as shown in Fig. 9a. The tensile strength of welded joints was

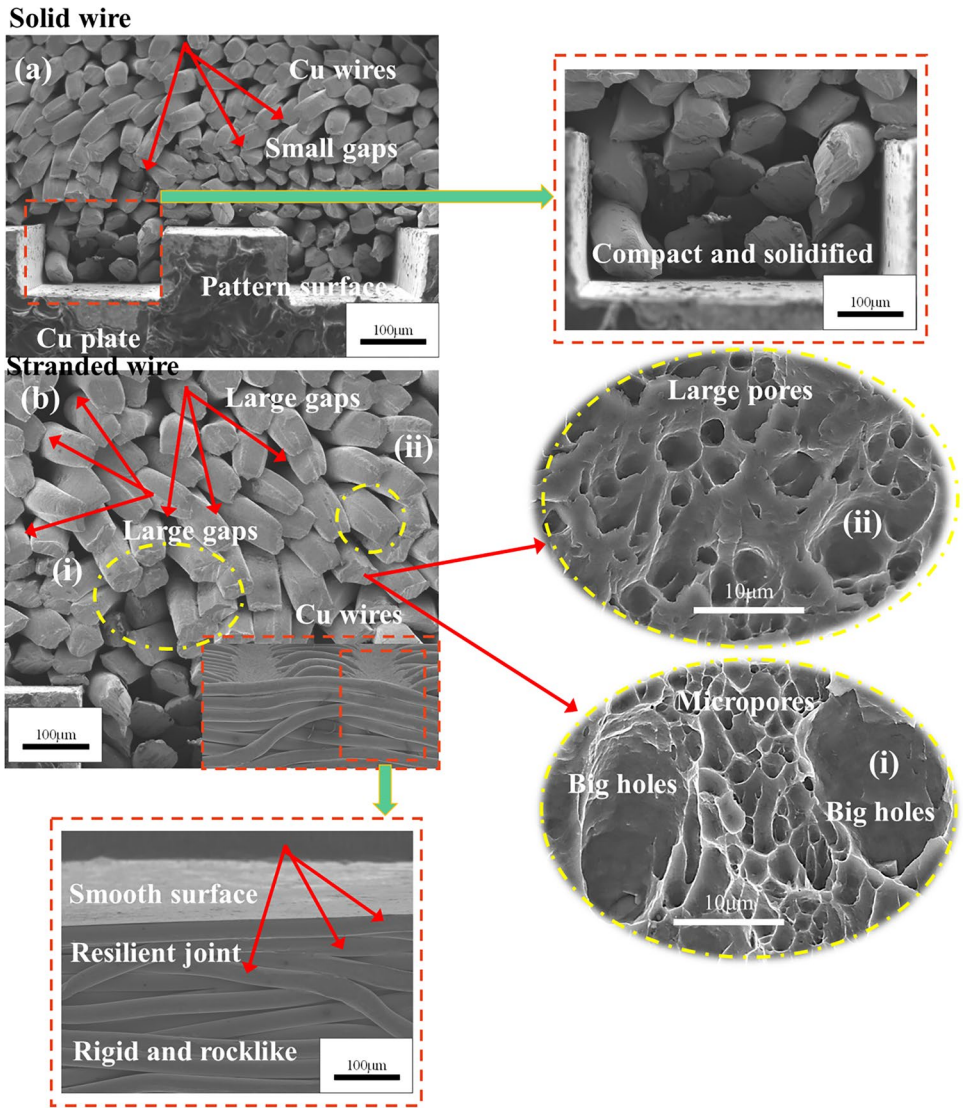

Fig. 9 SEM analysis of S4 substrate to conform the strength mode: **a** cross sectional analysis of vertical five-line patterns (S4) and **b** cross sectional analysis of minor and large gaps in wire harness

achieved with the highest welding energy absorption (e.g., 6000J–7000J). The soldered connection between the substrate and the wire on the vertical five-line surface is used to lead a stable and uncontaminated terminal (5021.2N) under instantaneous time intervals (e.g., 0.2 s). The SEM analysis was carried out to explore the superior performance of the welded joint according to the width of the centerline eutectic borides.

The compactness of the wire harness is strongly observed which increases the strength of the welded joint as shown in Fig. 9a. The strength of the soldered joint is non-glutinous in solid wire. Since, the substrate and wire were welded under the instantaneous effect of ultrasonic vibration. The results revealed that a large amount of vibrational energy is exerted on the surface of the upper side of the solid wire. So it generates a large degree of friction between the lower side of the wire and the upper side of the substrate. Figure 9b demonstrates tiny flaws, minor and large gaps between the stranded wires. However, the surface of the welded joints showed that the flaws and large gaps definitely weakened the joint due to greater impact of the ultrasonic vibration energy. In addition, micropores are observed in the top view of wire below 10 μm in size and large voids/gaps were found in the stranded wire welded joint which can break and produce an unstable joint. The selected area is subjected to a greater force and the stiffness is more serious. Thus, a small number of semi-elliptical cracks are distributed in the lower area of the wire which is created by the action of shear stress and belongs to the shear fracture. The SEM analysis indicated a firm welded joint between the wire strands and the copper substrate. The poor connection indicated by the gaps in S1, S2 and S5 was observed due to the poor ductility and bulging effect in the wire harness. It confirms the findings of the wire and substrate cross-sections. Therefore, a uniform

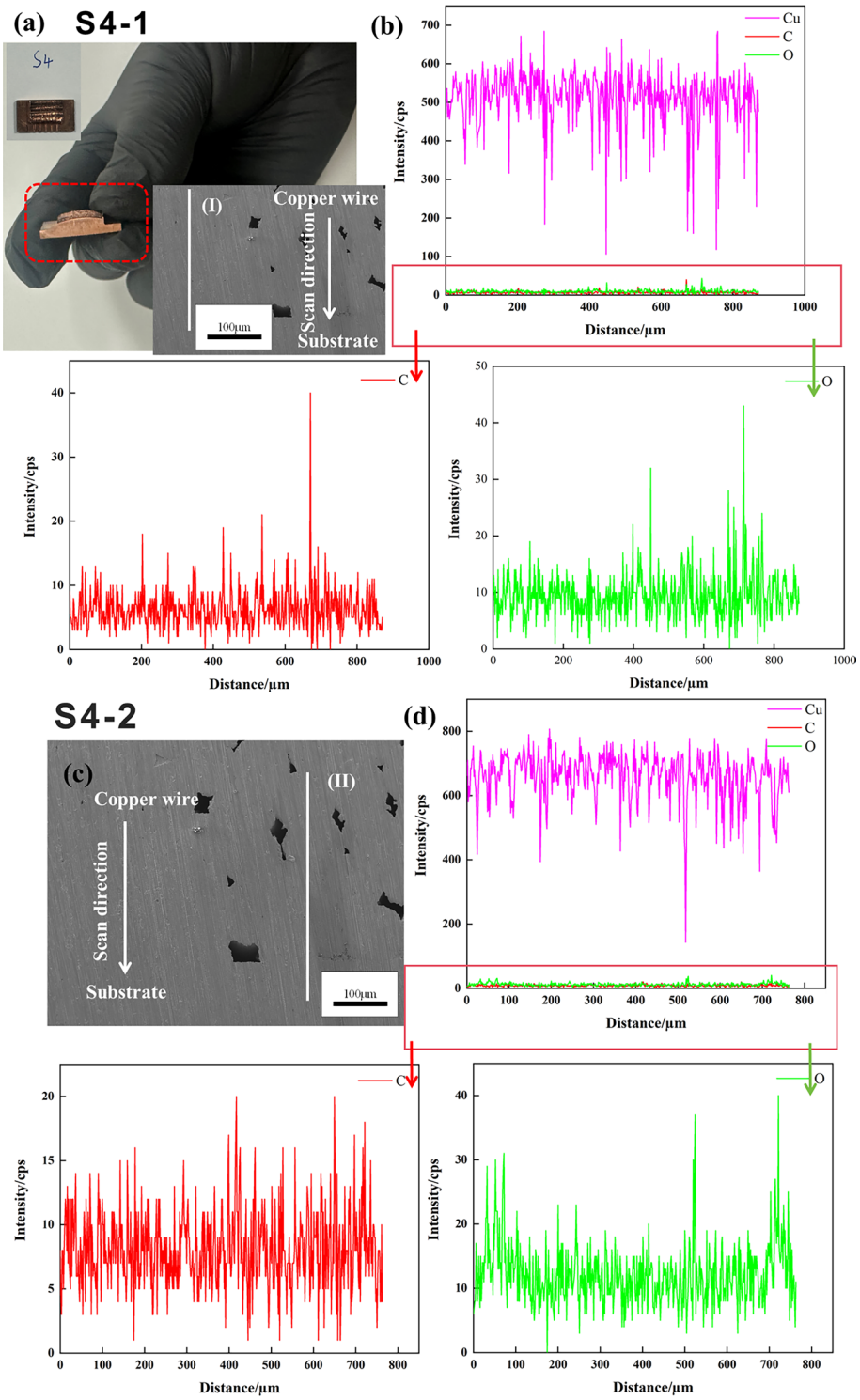

Fig. 10 Line scanning approach SEM–EDS analysis of S4 substrate to probe weight percentage of different elements: **a**, **b** EDS analysis of S4 by scanning side shape of groove (S4-1) and **c**, **d** SEM–EDS analysis of S4 by scanning internal lateral shape of the groove (S4-2)

and continuous layer of flake-like reaction between the wire and the copper plate is produced under vibration amplitude of 85%. The thickness of the smooth and stable layer was measured to 50 μm. It was formed in the interfacial area of the substrate. It can be concluded that the welded joint was initially resilient near the edge. The lower side of the substrate strength mode is marked with a red arrow in the photograph.

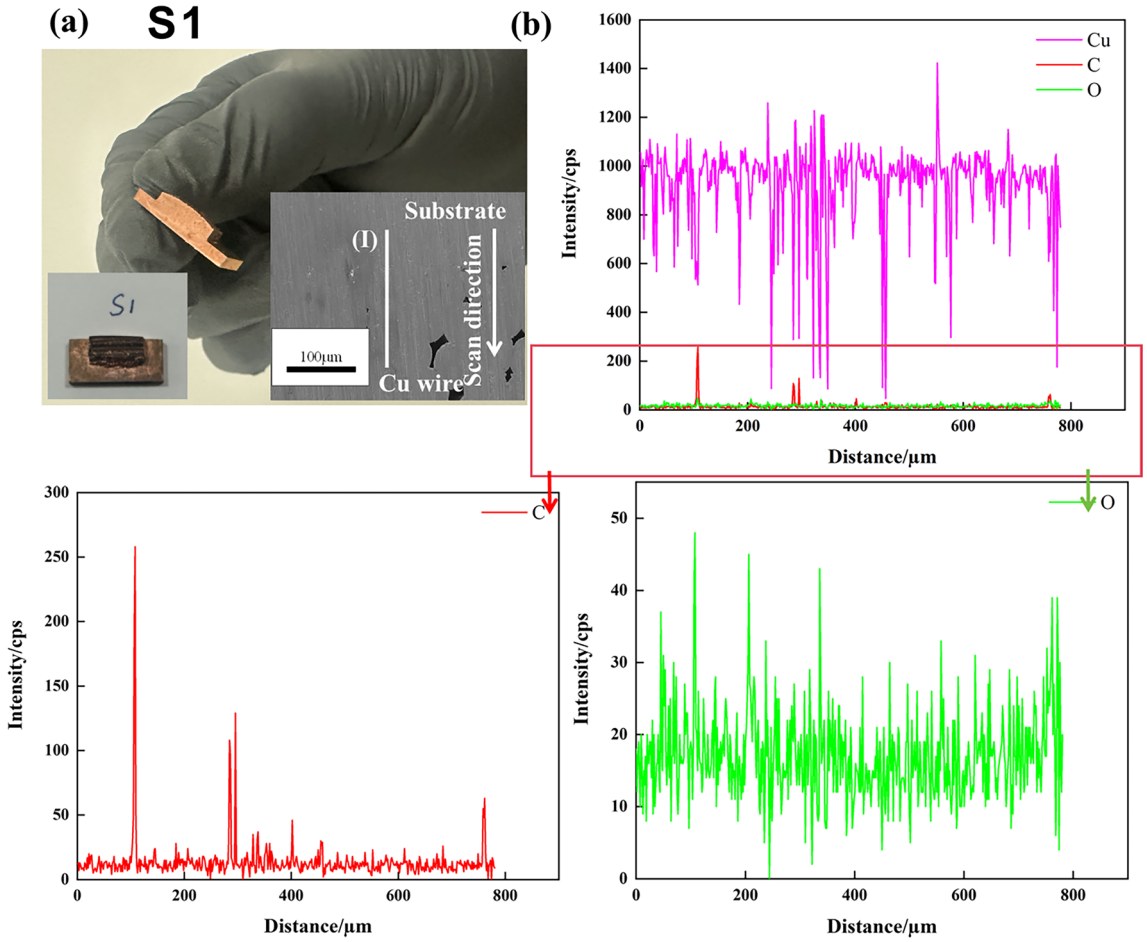

Fig. 11 Line scanning approach SEM–EDS analysis of S1 substrate to probe weight percentage of different elements: **a** cross-sectional analysis of junction between Cu wire and substrate, **b** The elemental analysis of the junction,

3.3 SEM–EDS Analysis

3.3.1 Elemental Analysis of Line and Point Scan Measurements

Figure 10 illustrates the cross-sectional areas of welded joint subjected to SEM–EDS under the line location scanning approach, i.e., base, joint and wire. The substrate S4 presents the shape of a groove as shown in Fig. 10a–d. The EDS analysis was performed on the side of the groove (S4-1) and internal lateral shape of the groove (S4-2), respectively. The combination of the two surfaces is set at 200 μm and 600 μm, respectively. Regularly, the Cu content decreased in the surface combination while the C and O content increased. So the strength was also weaker than the substrate and the Cu wire in the combination of the two groove cross-sections. The results of the S1 EDS scan measurement are shown in Fig. 11a, b. The line scan is taken from the intersection of the welded surface at about 400 μm. the analysis shows that the Cu content in the junction is decreased while the C and O contents are increased. This proves that the strength of welded joint at junction is weaker than the substrate and Cu wire. Similarly, the SEM–EDS analysis of S4 by scanning internal lateral shape of the groove (S4-2) is demonstrated in Fig. 10c, d.

Figure 12a illustrates the cross-sectional areas of the S1 substrate subjected to SEM–EDS under the point location scanning approach e.g., base, joint and wire. The highest concentration of Cu elements was found in the base site compared to other sites, which lead to the prediction of high strength of the welded joint. The high concentration of pure copper (Cu) elements on the base surface is 67% under the sigma weight of 1% as shown in Fig. 12b. The main reason is that the terminal mainly generates high frequency with copper wire on the surface during the welding process. So there can be only a very small amount of oxides and impurities are dislodged by friction on the terminal side. Therefore, the content of the welded joint is dissimilar on different location when performed using EDS measurement analysis. The analysis determined that the copper content decreases from

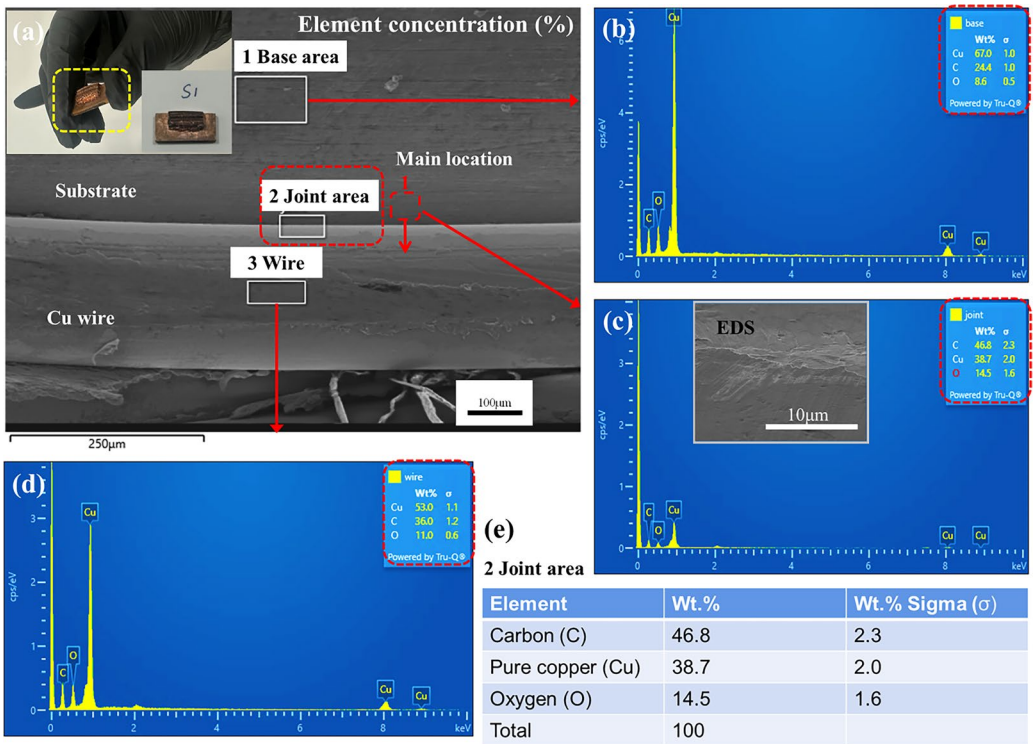

Element	Wt.%	Wt.% Sigma (σ)
Carbon (C)	46.8	2.3
Pure copper (Cu)	38.7	2.0
Oxygen (O)	14.5	1.6
Total	100	

Fig. 12 Point scanning approach SEM–EDS analysis of S1 substrate to predict weight percentage of different elements on particular locations for welded joint: **a** cross sectional analysis of reference joint (S1), **b**, **c**, **d** the SEM–EDS result corresponded to the secondary phase marked by the gray rectangular of the copper substrate and wire and **e** EDS analysis using elemental *K*-lines for specific location on welded joint

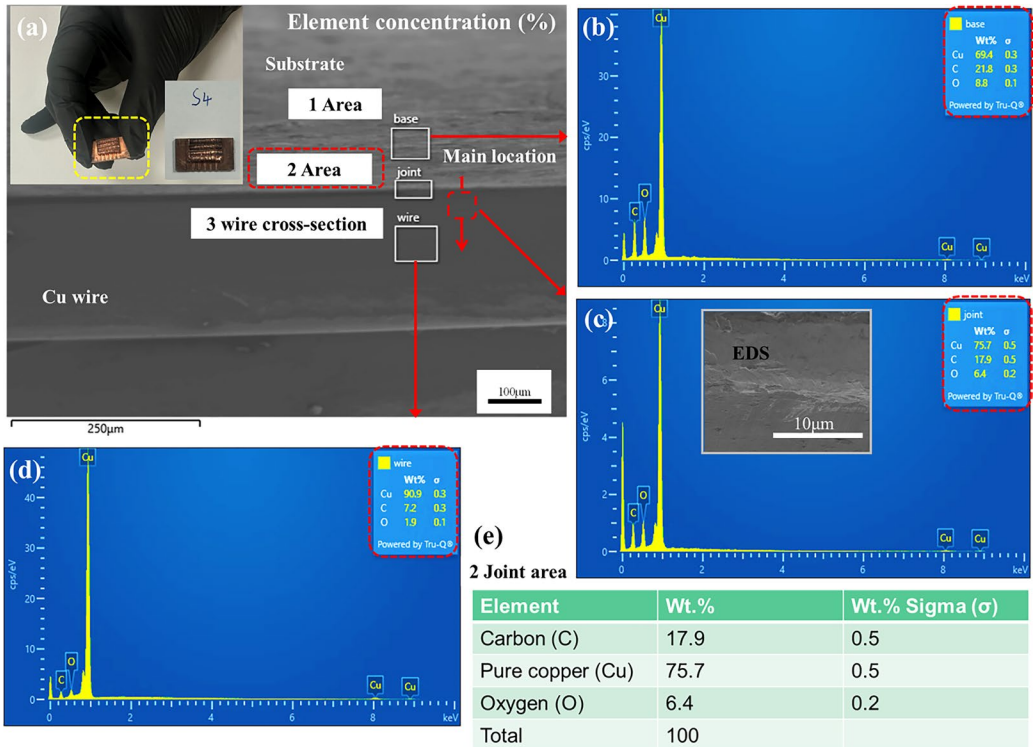

Element	Wt.%	Wt.% Sigma (σ)
Carbon (C)	17.9	0.5
Pure copper (Cu)	75.7	0.5
Oxygen (O)	6.4	0.2
Total	100	

Fig. 13 Point scanning approach SEM–EDS analysis of S4 substrate to predict weight percentage of different elements on base, joint and wire: **a** cross sectional analysis of S4 joint, **b**, **c**, **d** the SEM–EDS result corresponded to the secondary phase marked by the gray rectangular of the copper substrate and wire and **e** EDS analysis using elemental *K*-lines for specific location on welded joint

the wire to the junction point of the welded joint. This is because of the welding energy will decrease gradually from top to bottom during the welding process. So the friction and plastic deformation of the upper copper wire will be stronger than that of the lower copper. The wire will cause some oxides and impurities on the bottom layer to remain in a trivial amount. Therefore, it was investigated that the Cu content of the reference joint will be lower than that of the wire cable. During the SEM–EDS analysis for carbon content at the joint site, the reference joint of the substrate (S1) contains 46.8% as shown in Fig. 12c. This is due to the particles on the junction surface of the joint line were compacted to form major boundaries around the substrate. The size of the microstructures was estimated to be lower than 10 µm in the welded joint area. Thus, the resistance between the molecules increases under the rapid effect of the higher frequency. Similarly, the concentration of different elements has a different effect on different locations of the surface due to the specific plastic deformation under the applied load. In the case of the S1 substrate, the position of the welded joint may contain oxides and impurities of this fraction that may lead to an increase in the carbon content. Similarly, increasing the amount of carbon causes the stability to fluctuate and weaken the welded joint. Figure 12d shows the corresponding SEM–EDS results with the secondary phase for the copper substrate and wire, which investigated 53% Cu content. The EDS analysis using elemental *K*-lines for a specific location in welded joint is shown in Fig. 12e.

The SEM–EDS analysis of particular cross-sections in S4 substrate is carried out as shown in Fig. 13a. The concentration of element was investigated in different locations. Figure 13c shows 75.7% Cu content in five-row vertical welded joint compared to the reference joint. Thus, SEM–EDS analysis of S4 substrate was used to predict the weight percentage of various elements when the sigma weight was 0.5%, 0.5%, and 0.2%, respectively. In the case of S4 substrate, the position of the welded joint contains 17.9% carbon content that exhibits less oxides and fraction impurities. It can lead to increase stability and strengthening of the welded joint. Figure 13b, d shows the corresponding SEM–EDS results with the secondary phase as marked by gray rectangle. Figure 13e shows the EDS analysis using elemental K lines for the specific location in S4 joint. The wire cable displays a huge difference of Cu content in reference substrate (S1 = 53.0%) compared to the pattern substrate (S4 = 90.9%). The difference is identified due to the morphologies of straight line patterns that generate and increase frictional heat at the interface of the patterns. The increase in thermal energy at the interface reduces surface friction and squeezes the metal molecules within the wire rope. Finally, the SEM–EDS analysis demonstrates that the Cu content in the S4 joint is more than the S1 joint. It predicts and proves that the higher the Cu concentration at the joint site, the stronger the welded joint.

Ultrasonic metal welding technology is extremely useful and finds applications in many industries, including aerospace, batteries and electric vehicles. This paper reports ultrasonic welding tests between copper wire and copper plate. New pattern morphologies are machined into substrates to explore its influence on the mechanical properties of the welded joint. Patterns are divided into three different categories such as original surface, vertical pattern and horizontal pattern. The main reason for the development of pattern shapes was to overcome the challenges of lower force output, increased oxidation between two similar materials, the creation of corrosion layers and reduced durability of the welded joint. Cracking, microstructure strength and tensile properties of the welded joint are studied to improve the strength of welded joint. Moreover, the coupling mechanism of the processing method is analyzed. The results revealed that the joint performance of the vertical pattern (S4) was significantly improved + 15% through tensile tests compared to the reference substrate (S1) while the joint performance of horizontal pattern (S5) was relatively poor -16%. Optical microscopic analysis investigates the formation of additional bonding between multiple Cu wires while maintaining the compact properties of S4 substrate. The failure mode of the joint is obtained due to poor ductility or rupture of the welded joints in vertical three-line model where there are no plastic deformation phenomena. Similarly, the three-row zigzag pattern welded vertical joint caused the failure of deep cylindrical holes. Horizontal joints with three-row zigzag pattern generated swelling effect failure phenomena where the joint morphology swells and increases the size of the wires in top view. SEM–EDS point and line scan analysis was carried out. The results investigated that the maximum content of a Cu element was found in S4 (75.7%). However, in the S1 weld zone, 38.7% carbon content was estimated which can weaken the welded joint and reduce the stability of internal microstructures. The measurement direction of the soldered joint was chosen from the copper wire to the interface site. Furthermore, by evaluating mechanical properties of the materials produced in each refining process with this EDS analysis method, the verification work of the material for substrate S4 becomes very easy and simple. It was further verified that less cracks propagation damage is occurred in some parts of the welded joint during tensile testing which prove the credibility of our experiments.

4 Conclusions

The welded joints of EVR252 stranded wires with a cross section of 10 mm^2 and copper terminals were produced via ultrasonic metal welding. The oscillations of the stranded

wire, terminal, and anvil as well as the horn were measured. Then, welding was performed by increasing the welding time from 0.2 to 1.5 s in order to observe the wire consolidation, the morphological influence of the pattern, the joint shear strength and the mechanical properties of the interface as a function of welding time.. The following conclusions can be drawn from the aforementioned tests:

1. In this work, the novel pattern morphologies were proposed and developed on substrate surfaces to investigate the mechanical properties of the substrate-wire harness welded joint. To characterize the mechanical properties of the welded joint, the tensile tests were carried out. The results were compared with the original substrate (S1). It was investigated that the failure load of transverse pattern (3461N) was reduced. In contrast, the vertical 5-line pattern (S4 = 4755N) had approached best stability effect. Moreover, its failure load, failure displacement and energy absorption value are increased by 15%, 87% and 113%, respectively.
2. It was observed that the only small portion of the solder joint existed between Cu wire and horizontal pattern. Conversely, Cu wire and vertical 5-line pattern not only form a quality welded connection, but also increase the total surface area of weld under formation of joint morphology. Thus, the mechanical properties are increased under the higher welding energy effect in vertical 5-line pattern (S4).
3. The failure modes of the welded joint were exclusively analysed. It has been examined that the main modes of welded joint failures are as follows:
4. 1-poor ductility or rupture (no deformation) failure in vertical 3-line pattern joints, 2-cylindrical deep holes failure in vertical 3-line zigzag pattern joints and 3-bulging influence failure in horizontal 3-line zigzag pattern joints.
5. To summarize, the EDS point and line scan measurement analysis was performed for welded joints of S1 and S4. It has been investigated that the content of Cu element is decreased by Cu wire in joining direction of the welding place. Similarly, the content of Cu element in welded joint S4 was higher than that of joint S1.
6. The oxides and impurities from pure Cu were exposed due to grinded and polished cross-sections, which became the main cause for increasing carbon content in welded joint area. However, the strength of both joints was weaker than that of Cu wire and the substrate.
7. This study further investigated the welding strength of 5-line vertical joint (S4 = 5021.2N) which was maximum compared to 3-line vertical joint (S2 = 4712.65N). So, the welded joint S4 has endured more mechanical properties than joint S1 when the tensile test is performed.

5 Recommendations and Future Trends

A wire-harness and sheet welded joint is used for power transmission in automobiles, for telecommunication signals or to carry electricity and several other engineering applications. Future research should focus on new frameworks and refined feature estimation methods. The purpose of this study is to analyze the shortcomings and strengths of the state-of-the-art development process in the ultrasonic harness industry. It can minimize the challenges in evaluating feature distribution, simplify the process method, reduce oxidation at the interface of the welded joint, and increase its adaptability and durability in new environments. Additionally, the implementation of new patterns may allow and highlight some USW directions for future research on the correlation between pattern design, variability, and virtual instruments.

Acknowledgements This research is supported by National Natural Science Foundation of China (Grant No. 12104324); Postdoctoral Science Foundation of China (No. 2021M703392); Scientific Research Startup Fund for Shenzhen High-Caliber Personnel of SZPT (No.6022310046K); Postdoctoral Startup Fund of Shenzhen Polytechnic University (No. 6021330001K and No. 6022331008K).

Authors' contributions ZA and ZL, methodology, validation, investigation, formal analysis; ZA and FT, writing-original draft, writing-review and editing, visualization; ZA and FT, investigation, and formal analysis; ZA and ZL: conceptualization, methodology, validation, resources, visualization; ZL: supervision, project administration, funding acquisition; ZA, and MSI: writing-review and editing. All authors read and approved the final draft of the manuscript.

Data availability The datasets used and/or analyzed during the current study are available from the corresponding author upon reasonable request.

Declarations

Conflict of interest The authors declare that they have no known competing financial interests or personal relationships that could have appeared to influence the work reported in this paper.

Ethical approval Not applicable.

Approval for animal experiments Not applicable.

Consent to participate Not applicable.

Consent for publication Not applicable.

References

1. E. Riedel, M. Liepe, S. Scharf, Simulation of ultrasonic induced cavitation and acoustic streaming in liquid and solidifying aluminum. Metals (Basel) **10**, 476 (2020). https://doi.org/10.3390/met10040476
2. M.P. Matheny, K.F. Graff, *Ultrasonic Welding of Metals* (Elsevier Ltd, Amsterdam, 2015)
3. A. Gester, G. Wagner, P. Pöthig et al., Analysis of the oscillation behavior during ultrasonic welding of EN AW-1070 wire strands and EN CW004A terminals. Weld. World **66**, 567–576 (2022). https://doi.org/10.1007/s40194-021-01222-z
4. H. Huang, J. Chen, Y.C. Lim et al., Heat generation and deformation in ultrasonic welding of magnesium alloy AZ31. J. Mater. Process. Technol. **272**, 125–136 (2019). https://doi.org/10.1016/j.jmatprotec.2019.05.016
5. A. Levy, S. Le Corre, I. Fernandez Villegas, Modeling of the heating phenomena in ultrasonic welding of thermoplastic composites with flat energy directors. J. Mater. Process. Technol. **214**, 1361–1371 (2014). https://doi.org/10.1016/j.jmatprotec.2014.02.009
6. D. Zhao, K. Zhao, D. Ren, X. Guo, Ultrasonic welding of magnesium-titanium dissimilar metals: a study on influences of welding parameters on mechanical property by experimentation and artificial neural network. J. Manuf. Sci. Eng. **139**, 031019 (2017). https://doi.org/10.1115/1.4035539
7. F. Rubino, H. Parmar, V. Esperto, P. Carlone, Ultrasonic welding of magnesium alloys: a review. Mater. Manuf. Process. **35**, 1051–1068 (2020). https://doi.org/10.1080/10426914.2020.1758330
8. C. Liu, Y. Gong, Y. Wang et al., Preparation and characterization of wear resistant TiO layer on Ti alloy. Surf. Coat. Technol. **470**, 129833 (2023). https://doi.org/10.1016/j.surfcoat.2023.129833
9. S.S. Ao, M.P. Cheng, W. Zhang et al., Microstructure and mechanical properties of dissimilar NiTi and 304 stainless steel joints produced by ultrasonic welding. Ultrasonics **121**, 106684 (2022). https://doi.org/10.1016/j.ultras.2022.106684
10. S.K. Bhudolia, G. Gohel, K.F. Leong, Advances in ultrasonic welding of thermoplastic composites: a review. Materials **13**, 1284 (2020). https://doi.org/10.3390/ma13061284
11. J. Liu, B. Cao, J. Yang, Effects of vibration amplitude on microstructure evolution and mechanical strength of ultrasonic spot welded Cu/Al joints. Metals (Basel) **7**, 471 (2017). https://doi.org/10.3390/met7110471
12. D. Zhao, C. Jiang, K. Zhao, Ultrasonic welding of AZ31B magnesium alloy and pure copper: microstructure, mechanical properties and finite element analysis. J. Mater. Res. Technol. **23**, 1273–1284 (2023). https://doi.org/10.1016/j.jmrt.2023.01.095
13. D. Zhao, W. Wang, D. Ren, K. Zhao, Research on ultrasonic welding of copper wire harness and aluminum alloy: based on experimental method and GA-ANN model. J. Mater. Res. Technol. **22**, 3180–3191 (2023). https://doi.org/10.1016/j.jmrt.2022.12.155
14. Z. Du, L. Duan, L. Jing et al., Numerical simulation and parametric study on self-piercing riveting process of aluminium–steel hybrid sheets. Thin-Walled Struct. **164**, 107872 (2021). https://doi.org/10.1016/j.tws.2021.107872
15. Z. Lun, W. Shicheng, L. Jiguang et al., Performance enhancement of clinched joints with ultrasonic welding for similar and dissimilar sheet metals. Weld. World **12,** 2715–2729 (2023). https://doi.org/10.1007/s40194-023-01589-1
16. H. Li, B. Cao, J.W. Yang, J. Liu, Modeling of resistance heat assisted ultrasonic welding of Cu–Al joint. J. Mater. Process. Technol. **256**, 121–130 (2018). https://doi.org/10.1016/j.jmatprotec.2018.02.008
17. J. Saleem, A. Majid, K. Bertilsson et al., Nugget formation during resistance spot welding using finite element model. Int. Sch. Sci. Res. Innov. **6**, 707–712 (2012)
18. P. Pöthig, M. Grätzel, J.P. Bergmann, Influence of different surface conditions on mechanical properties during ultrasonic welding of aluminum wire strands and copper terminals. Weld. World **67**, 1427–1436 (2023). https://doi.org/10.1007/s40194-023-01490-x
19. D. Zhao, D. Ren, K. Zhao et al., Ultrasonic welding of magnesium-titanium dissimilar metals: a study on thermo-mechanical analyses of welding process by experimentation and finite element method. Chin. J. Mech. Eng. (English Ed) **32**, 97 (2019). https://doi.org/10.1186/s10033-019-0409-8
20. J. Tsujino, S. Ihara, Y. Harada et al., Characteristics of coated copper wire specimens using high frequency ultrasonic complex vibration welding equipments. Ultrasonics **42**, 121–124 (2004). https://doi.org/10.1016/j.ultras.2004.01.051
21. X.M. Cheng, K. Yang, J. Wang et al., Ultrasonic welding of Cu to Al cables bonding: evolution of microstructure and mechanical properties. Mater. Charact. **200**, 112905 (2023). https://doi.org/10.1016/j.matchar.2023.112905
22. Z. Liu, S. Ji, X. Meng, Joining of magnesium and aluminum alloys via ultrasonic assisted friction stir welding at low temperature. Int. J. Adv. Manuf. Technol. **97**, 4127–4136 (2018). https://doi.org/10.1007/s00170-018-2255-8
23. J. Li, J. Zillner, F. Balle, In-depth evaluation of ultrasonically welded Al/Cu joint: plastic deformation, microstructural evolution, and correlation with mechanical properties. Materials **16**, 3033 (2023). https://doi.org/10.3390/ma16083033
24. H. Ji, J. Wang, M. Li, Evolution of the bulk microstructure in 1100 aluminum builds fabricated by ultrasonic metal welding. J. Mater. Process. Technol. **214**, 175–182 (2014). https://doi.org/10.1016/j.jmatprotec.2013.09.005
25. S.H. Kang, H.K. Kim, Fatigue strength evaluation of self-piercing riveted Al-5052 joints under different specimen configurations. Int. J. Fatigue **80**, 58–68 (2015). https://doi.org/10.1016/j.ijfatigue.2015.05.003
26. S. Lu, D. Wu, M. Yan, R. Chen, Achieving high-strength and toughness in a Mg–Gd–Y alloy using multidirectional impact forging. Materials (Basel) **15**, 1508 (2022). https://doi.org/10.3390/ma15041508
27. S. Kumar, C.S. Wu, G.K. Padhy, W. Ding, Application of ultrasonic vibrations in welding and metal processing: a status review. J. Manuf. Process. **26**, 295–322 (2017). https://doi.org/10.1016/j.jmapro.2017.02.027
28. K.J. Pradeep, K. Prakasan, Acoustic horn design for joining metallic wire with flat metallic sheet by ultrasonic vibrations. J. Vibroeng. **20**, 2758–2770 (2018). https://doi.org/10.21595/jve.2018.19648
29. M. Schramkó, Z. Nyikes, H. Jaber, T.A. Kovács, Dissimilar joining by ultrasonic welding. J. Hunan Univ. Nat. Sci. **49**, 185–191 (2022). https://doi.org/10.55463/issn.1674-2974.49.3.20
30. R.P. Singh, S. Dubey, A. Singh, S. Kumar, A review paper on friction stir welding process. Mater. Today Proc. **38**, 6–11 (2020). https://doi.org/10.1016/j.matpr.2020.05.208
31. P. Pöthig, M. Grätzel, J.P. Bergmann, Influence of different surface conditions on mechanical properties during ultrasonic welding of aluminum wire strands and copper terminals. Weld. World **67**, 1427–1436 (2023). https://doi.org/10.1007/s40194-023-01490-x
32. A. Ben Khalifa, S. Braiek, A. Fradj, M. Trigui, Experimental investigation of joints strength obtained by ultrasonic welding and soldering under pure T-peel tests using DIC. Weld. World **67**, 495–511 (2023). https://doi.org/10.1007/s40194-022-01437-8

33. H. Lu, F. Ye, Y. Wang, Orthogonal experiments and bonding analysis of ultrasonic welded multi-strand single core copper cables. J. Manuf. Process. **78**, 1–10 (2022). https://doi.org/10.1016/j.jmapro.2022.04.007
34. F. Ye, H. Lu, H. Qi, Joints formation and bonding mechanism of ultrasonic welded multi-strand single core copper cables with copper terminals. Mater. Lett. **327**, 133015 (2022). https://doi.org/10.1016/j.matlet.2022.133015
35. M.P. Satpathy, S.K. Sahoo, Microstructural and mechanical performance of ultrasonic spot welded Al-Cu joints for various surface conditions. J. Manuf. Process. **22**, 108–114 (2016). https://doi.org/10.1016/j.jmapro.2016.03.002
36. C.B.G. Brito, J. Teuwen, C.A. Dransfeld, I.F. Villegas, The effects of misaligned adherends on static ultrasonic welding of thermoplastic composites. Compos. Part A Appl. Sci. Manuf. **155**, 106810 (2022). https://doi.org/10.1016/j.compositesa.2022.106810
37. Z.M. Su, P.C. Lin, W.J. Lai, J. Pan, Fatigue analyses of self-piercing rivets and clinch joints in lap-shear specimens of aluminum sheets. Int. J. Fatigue **72**, 53–65 (2015). https://doi.org/10.1016/j.ijfatigue.2014.09.022
38. L. Zhao, X. He, B. Xing et al., Fracture mechanism of titanium sheet self-piercing riveted joints. Thin-Walled Struct. **144**, 106353 (2019). https://doi.org/10.1016/j.tws.2019.106353